Modelling of the Optical Detector System in a Compact Disc Player Servo System

P.F. Odgaard, J. Stoustrup, P. Andersen
Department of Control Engineering
Aalborg University
DK 9220 Aalborg
{odgaard,jakob,pa}@control.auc.dk

H.F. Mikkelsen
Bang & Olufsen a/s
Peter Bangs vej 15
DK 7600 Struer
hfm@bang-olufsen.dk

Abstract

The cross-couplings between focus and radial tracking servos in compact disc players are important, but the optical cross couplings are not well described in the literature. In this paper an optical model of a compact disc player based on the three beam single foucault detector principle is found. The general principle of the three beam focus and radial detector system is first described, followed by a non-linear static model of the relationship between the detector signals as outputs and focus and radial errors as inputs. The parameters in these models are found by using actual data from a Compact Disc player, and the model is validated by comparing the simulated model response to the measured system response to a given set of inputs. This validation shows that the derived model gives a good and usable description of the optical three beam single foucault detector system in a Compact Disc player, which includes the cross couplings between focus and radial loops.

1. Introduction

One of the main characters of Compact Disc players (CD players) is the absence of physical contact between the optical pick-up and the disc surface. Instead two servo control loops are implemented to keep the pick-up focused at the disc surface and to keep the pick-up radially tracked. A three beam optical detector system is used to achieve radial and focus sensor signals. The detector system has some cross couplings. The actuators in both loops are electro-magnetic actuators which are placed orthogonally to each other and should thereby be decoupled. However, in practice they are not totally decoupled. The cross-couplings can be divided into three different groups of interactions: mechanical, electro-magnetic and optical exist [1]. Models of these interactions are needed to achieve a MIMO servo controller which can handle these interactions. Modelling the optical part of CD player servos is also interesting in another perspective, in the task of detecting and handle disc abnormalities such as scratches. An interesting method is to measure the distance of a given sample of sensor signals to a set in which the samples would be if no abnormalities occur. This set can be found by the models of the optical detector system, which map from focus and radial error to focus and radial sensor signals.

A large amount of work is performed in modelling and identification of the mechanical and electro-magnetic parts of CD players. [2] focus on the modelling of these parts of the system and [3] describes a simple method to perform open loop system identification. Both [4] and [1] perform some work on the cross-couplings in the mechanical and electro-magnetic parts between focus and radial loop. Regarding the optical part of the system the present control strategies are based on simple linear models not concerning the optical cross coupling [2] and [5], although some work has been done regarding the optical model. [4] has some considerations about the optical cross-couplings. [6] and [7] deals with models of the optical signal of focus error without consideration about the cross coupling with the radial loop. This model is used for detection of surface defects on the disc. The principle behind the optical pick-up applied in this work is the single foucault three beam principle, which is described in [5], [2]. Based on these principles and measurements on CD player test setup, a model is made of a three beam single foucault optical detector system. This model maps from focus and radial errors, to focus sensors and radial sensor signals, and include the cross-couplings between focus and radial loops.

In the following the general principle of an optical detector system based on the three beam single foucault principle is presented, followed by the modelling of this optical detector system. A non-linear static model is derived. The parameters in the model are next identified based on measurements on an experimental rig. Using these identified parameters in the model, the model response is compared with a system response on the same input signal. Finally these results are compared, and it is concluded that the derived model is well suited for control and fault detection purposes.

2. The three beam single foucault detector principle

In the CD player, used in this work, the main beam is used both to restore the information saved on the disc, and to focus the beam at the disc reflection layer. Two additional beams are used to keep the main beam radially tracked at the track. The information in the track is stored by using two different levels, called pit and land, (the land has the same level as the area between the tracks). The level difference is a quarter of the wave length of laser beam. I.e. when the light is reflected, the light reflected from a pit interferes destructively with the light reflected from a land. These pits and lands are also important in the task of modelling the optical models of the system. In the following focus and radial detector principles are briefly described.

2.1. The focus detector

The focus detector consists of two detector signals, D_1 and D_2. The idea is to introduce some asymmetry in the light path from the disc surface to these detector in such a way, that if the light beam is focused $D_1 - D_2 = 0$, and if the pick-up is too far away from the disc $D_1 - D_2 > 0$, and if it is too close $D_1 - D_2 < 0$. This asymmetry can be generated in a number of ways, e.g. by the single foucault principle which is illustrated in Fig. 1. The idea behind this focusing principle

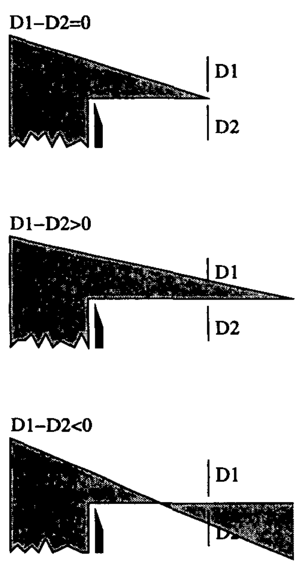

Figure 1: Illustration of the single foucault focus detector principle.

is to place a knife into the light path, such that only half of the light beam passes the knife, and the rest is absorbed by the knife. The optical system is designed in such a way that if the light beam is focused on the disc it will also be focused on the detectors. In the cases where the pick-up is either too close to or too far away from the disc, the beam focus point would be either behind or in front of the detectors. The principle

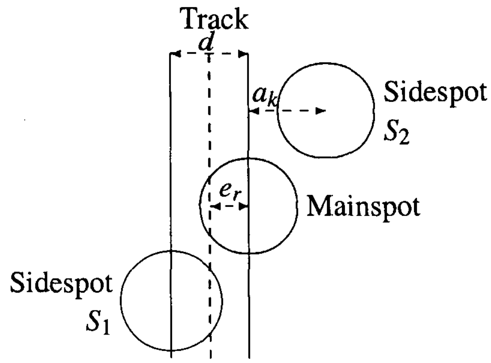

Figure 2: Illustration on how the three beams are placed to each other on the disc surface.

illustrated in Fig. 1 is based on the assumption that the light is emitted from a point source. A better description of the source, however, is to consider it as a disc. This results in that the light is detected on both D_1 and D_2 in all situations, but the sign of the difference between D_1 and D_2 is the same as in Fig. 1.

2.2. The radial detector

Fig. 2 illustrates how the three beams are placed relative to each other on the disc surface. The main spot in the middle and the two others are placed one to each side of the track, with a distance from their centre to the middle of the track called a_k. If the pick-up is located symmetrically over the track, the two side spots will cover equal areas of the track. Due to the fact that the disc spins around and that the detector signals are low-pass filtered, only the mean of pits and lands is seen in the detector signals. Fig. 2 illustrates a situation where the pick-up is too much to the right. In this case S_2 receives more light energy than S_1, due to the destructive interferences, I.e. $S_1 - S_2 < 0$. On the other hand if the pick up is too much to the left, $S_1 - S_2 > 0$.

3. The focus and radial models

Rather than only considering differences the four detector signals are modelled individually. This optical model is expressed by the mappings, described by (1-4).

$$f_1 : (e_f, e_r) \rightarrow D_1 \quad (1)$$

$$f_2 : (e_f, e_r) \rightarrow D_2 \quad (2)$$

$$f_3 : (e_f, e_r) \rightarrow S_1 \quad (3)$$

$$f_4 : (e_f, e_r) \rightarrow S_2 \quad (4)$$

Due to limitation in the test setup it is only possible to verify and identify parameters in the mappings if the following assumption about these mapping is used.

$$f_i(e_f, e_r) \approx h_i(e_f) \cdot g_i(e_r), \quad (5)$$

Proceedings of the American Control Conference
Denver, Colorado June 4-6, 2003

where

$$i \in \{1,2,3,4\}. \tag{6}$$

This assumption implies that the radii of the spots at the disc are constant, even though they depend on e_f. However, an increase in the actual area of the spot is not important for the model. The important thing is the ratio between the area of the spot covering the track, A_{trac}, and the area of the spot covering some of the area between the tracks, A_{CD}. This ratio is not varying much, and can as a consequence be neglected. After the parameters was identified this assumption was tested, by changing the radius of the spot, it was seen that these changes give little results on the values of $g_i(e_r)$. (5) can be interpreted as follows. The $g_i(e_r)$ function computes the maximal detected energy for a given value of e_r. $h_i(e_f)$ computes how large a ratio of the reflected energy in the spot which is detected.

3.1. Focus error to detector signals $h_i(e_f)$

The mappings $h_1(e_f)$ and $h_2(e_f)$ are related in the following way:

$$h_1(e_f) = h_2(-e_f), \tag{7}$$

due to the linear movement of the focus point relative to the detectors. As a consequence of (7) it is only needed to model one of these functions. This model of how e_f influence the detector signals consists of two parts. The first part is due to the single foucault principle. The light beam at the detector will be shaped as a half disc, due to the single foucault principle. The radius of the half disc, r, increases linearly with e_f. The detectors are relatively small due to the implementation and in order to minimise the noise received through the detectors. As a consequence the light beam covers more and more area outside the detector as e_f increases. This is the second part of the model.
Starting with the first part of the model, all the lenses in the light path from light source to the disc surface are merged into one lens, F. The distance from the lens to the disc surface and back to the lens again is l_x:

$$l_x = l_{x,0} - 2 \cdot e_f. \tag{8}$$

The distance from the source to the lens, l_u is:

$$l_u = l_{u,0} + c_f \cdot u_f. \tag{9}$$

Where: u_f is the control signal to the focus actuator. $l_{x,0}$, $l_{u,0}$ and c_f are a constants. The light source and detectors are placed at almost the same place so the light travels through the same lenses with focal width F. This means that by using the rules of thin lenses the focus point near the source and detector, F_l can be found by:

$$F_l = \frac{1}{\frac{1}{F} - \frac{2}{l_x}}. \tag{10}$$

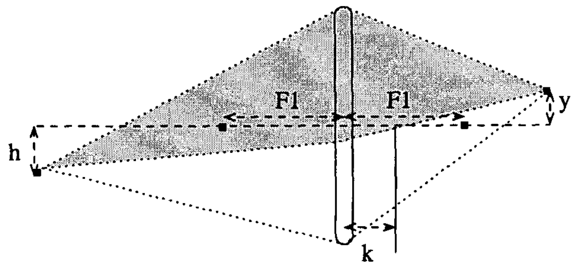

Figure 3: Illustration on how much light is absorbed by the knife.

The next step is to find how large a part of the energy sent from the source, which is detected at the detectors. The disc shaped source can be divided into lines with a given coordinate perpendicular to the knife edge, h. Fig. 3 illustrates how much of the energy sent from a point in the line which is received in a point in the line at the detector with the vertical coordinate y. The figure illustrates that light travelling in the gray area passed through to the detector. The cross section area at the lens of the beam that passes through is called A_l, the light spot at the lens has a radius R, and ratio of light detected relative to the emitted light is $\frac{A_l}{\pi \cdot R^2}$, and A_l is

$$A_l = \frac{1}{2} \cdot \pi \cdot R^2 + R^2 \cdot \arcsin(\frac{x}{R}) + x \cdot \sqrt{R^2 - x^2}, \tag{11}$$

where

$$x = \frac{k \cdot h}{l_m - k} \cdot \frac{F_l}{l_x - F_l}, \tag{12}$$

$$k = l_u - k_0, \tag{13}$$

$$l_m = \frac{l_u}{l_u - F_l} \cdot F_l. \tag{14}$$

By integrating the ratio over the whole half disc, ($[0; R_{source}]$), where R_{source} is the radius of the source. Part 1 of $h_1(e_f)$ is now found. This integration is done numerically by splitting the half disc up into approximation rectangles, and summing these, see [8]. Modelling the second part is to find the ratio of the light energy detected at the detector relative to the energy intended to be detected, η. The shape of the detector is assumed to be a rectangle ($b \times 2b$). Fig. 4 illustrates the three possible situation on how the reflected spot covers the detector. By inspecting Fig. 4, the expression of η can be found to be:

$$\eta = \begin{cases} 1 & \text{if a)} \\ \frac{\frac{1}{2} \cdot \pi r^2 - r^2 \cdot (2\theta_1 - \sin(2 \cdot \theta_1))}{\frac{1}{2} \cdot \pi r^2} & \text{if b)} \\ \frac{2 \cdot b^2}{\frac{1}{2} \cdot \pi \cdot r^2} & \text{if c),} \end{cases} \tag{15}$$

where

$$\theta_1 = \arccos(b/r), \tag{16}$$

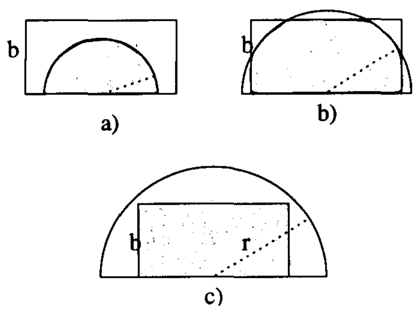

Figure 4: Illustration on how the reflected light covers the detector and area outside the detector as radius of the reflected half disc beam increases. a) $r < b$, b) $b \leq r \leq \sqrt{2 \cdot b^2}$ and c) $r > \sqrt{2 \cdot b^2}$

and a), b) and c) are defined in Fig. 4. $h_1(e_f)$ and $h_2(e_f)$ are now found, the next step is to find $h_3(e_f)$ and $h_4(e_f)$. The last two functions can be found by the same principle, which is described in the following. The side beams follow the same light path through the lenses as the main beam. However, the single foucault effect is not applied to the side detectors. Instead e_f influences the radial detector signals by the radius of the beam disc at the detector, and since more and more of light from the main spot is detected at the side detectors as e_f increases. This relationship is highly dependent on how the detectors are placed relative to each other, e.g. the size of the distance between the detectors. These sizes are not known by the authors. Due to this it is hard to model how much of the energy from the main spot, that is placed at the side detectors as e_f increases. Instead this part is approximated by a polynomial as a function of e_f. In Section 4 the parameters in the models are identified based on measurements. These two model parts are merged into one model, by using the polynomial for small values of e_f and using the other part for larger values of e_f, see [8].

3.2. Radial error to detector signals, $g_i(e_r)$

These functions model how much light energy in each of the light beams, that is reflected at the disc. The functions $g_1(e_r)$ and $g_2(e_r)$ relate both to the main spot, i.e. $g_1(e_r) = g_2(e_r)$. The two side spots are detected by it own detector, i.e. $g_1(e_r) \neq g_2(e_r) \neq g_3(e_r)$.

The principle in this model is basically that when the spot is moved over the track, by changing e_r, the area of the spot not covering the track, A_{CD} and the area of the spot covering the track, A_{track} are changed. By changing e_r in Fig. 2 all three spots can be moved to cover track and area between the track in different ratios. This means that the model of these three spots are the same except from a offset, a_k. So in the following only the main spot is modelled, $g_1(e_r)$, since $g_3(e_r) = g_1(e_r - a_k)$ and $g_4(e_r) = g_1(e_r + a_k)$. The track consists of both pits and lands, due to the facts that the detector signals are low-pass filtered and that the disc spins around. This can be modelled by taking the mean of the two situations occurring when the spot covers some of the track. It either covers some of a pit or a land. This means that $g_1(e_r)$ can be expressed as:

$$\begin{aligned} g_1(e_r) = & \frac{1}{2} \cdot ((1 + \frac{A_{track}(e_r)}{A}) \cdot \rho_{land}) \cdot E_{beam} \\ & - \frac{1}{2} \cdot (\frac{A_{track}(e_r)}{A} \cdot \rho_{pit}) \cdot E_{beam}, \end{aligned} \tag{17}$$

where: ρ_{land} and ρ_{pit} are the reflection ratios of a land and a pit. E_{beam} is the energy in the beam before it is reflected at the disc surface. $A_{track}(e_r)$ can be derived by inspection of Fig. 2 and by using the rules of areas of disc segments. The expression of $A_{track}(e_r)$ consists of five parts each supported in a interval of e_r and is as a consequence a quite large expression, which is therefore omitted in this paper. However, an extended version of this paper including the omitted equations, can be found on the WWW [8]. It is needed to make an adjustment to the model, due to the assumption regarding the uniform distribution of the light energy in sender. The model is corrected by convoluting the output with the bell shaped energy distribution, which can be seen in [2] and [5].

4. Measurements and parameter identification

The measurements are performed on a laboratory setup of the CD player connected to a PC through an I/O-card. This setup has the possibilities of measuring a number of signals and to control focus and radial servos. The setup is also described in [3]. The measurements of $f_i(e_f, 0)$ are performed by slowly changing the focus position. It is done by applying a slowly varying saw tooth signal as control signal, u_f, while the disc does not spin around. This signal is sampled with a frequency at 5 kHz. The measurements of the $f_i(0, e_r)$ are done while the disc spins around, and with an active focus controller but without radial radial control. Due to the eccentricity of the disc this will result in a harmonic movement of the pick-up relative to the disc surface. This signal is sampled with a frequency at 35 kHz. Only a part of this signal is used for parameter identification. It is the part where the pick-up crosses the track slowly. I.e. the derivative of the sine function is near to zero. The parameters in this sine function are identified along with the model parameters in the parameter identification. The first measurements are used for the identification of parameters in the $h_i(e_f)$ functions and the second set of measurements are used for $g_i(e_r)$. Before doing the identification the $h_i(e_f)$ and $g_i(e_r)$ are multiplied with a parameter representing the amplification in the detector and an offset is added to this also due to the detectors. The parameter identifications were done by using the Matlab function `fminsearch` to minimise the squared error of the difference between the measurements and model output, by changing the parameter. The initial parameters were found partly in [5] and partly by trial and error. The model obtained with the identified parameters is compared with the measurements in Figs. 5-11 as function of either $c \cdot e_f$ or e_r.

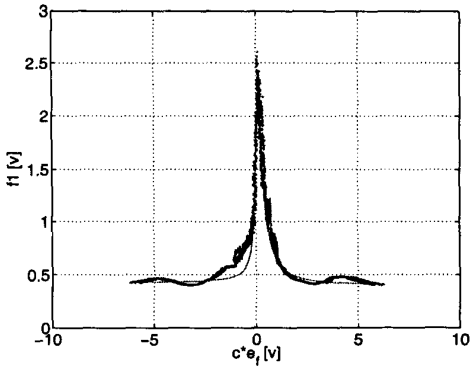

Figure 5: $f_1(c \cdot e_f, 0)$. The solid line is the simulation and the dotted line is the measurements.

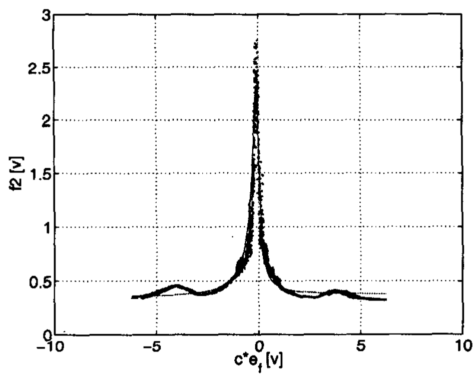

Figure 6: $f_2(c \cdot e_f, 0)$. The solid line is the simulation and the dotted line is the measurements.

5. Discussion

The Figs. 5-11 show how the models in general have highly similar responses to the given inputs as the optical system have. But due to some of the simplifications in the model/assumptions, the models do not describe all phenomena in the optical detector system. In Figs. 5, 6, 8 and 9 there are some bumps at approximately $|c \cdot e_{textf}| = 4\text{V}$, due to light from the other detector beams, which are not modelled. The size of the cross-couplings between the radial distance and the focus detectors can be seen in Fig. 7, e.g. the detector values increased with 7% if $e_r = 0.208\mu\text{m}$. The radial detectors signals increases with up to 37 % as e_f increases. By inspecting Figs. 10 and 11 it is seen that a low order polynomium could have been a good model instead. This means that the model can be simplified without loss of details by use of polynomiums as the $g_i(e_r)$ functions. This optical model is important since it spans a set in which the detector signals will be if only disturbances occurs. A given sample of detectors signals deviation from this set can be used for detection of disc defects since this defect can have caused the devia-

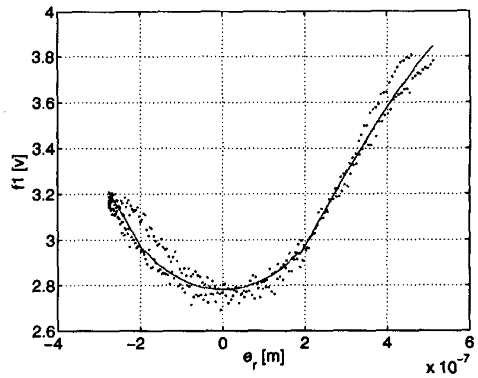

Figure 7: $f_1(0, e_r)$. The solid line is the simulation and the dotted line is the measurements.

tion. In this paper it is seen that the use of detector signals for control introduces important cross-couplings, a method to avoid these cross couplings is by solving the inverse problem of the model, I.e. by computing e_f and e_r based on the detector signals. e_f and e_r are decoupled and can following be used as feedback signals to the servo controllers.

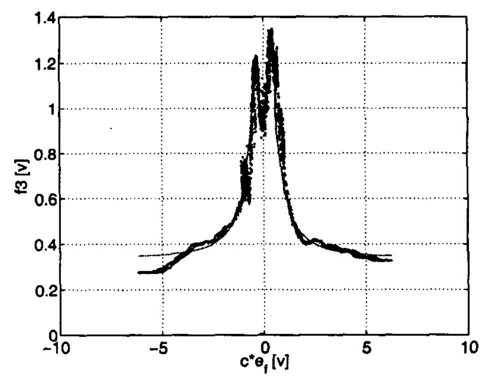

Figure 8: $f_3(c \cdot e_f, 0)$. The solid line is the simulation and the dotted line is the measurements.

6. Conclusion

In this paper a non-linear static model is found of a three beam single foucault detector system for compact disc players. This model is validated by comparison with actual data, and it is concluded that the model describes the important main trends of the measurements, and the model is thereby useful for control and fault detection.

7. Acknowledgement

The authors acknowledge the Danish Technical Research Council, for support to Peter Fogh Odgaard's Ph.D

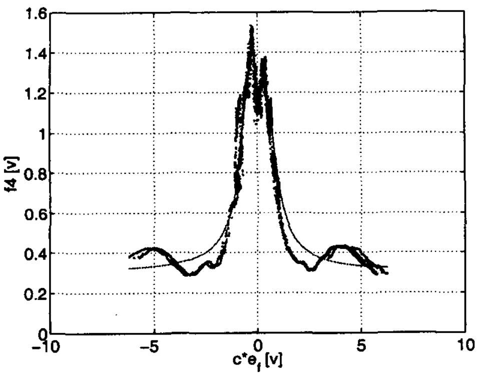

Figure 9: $f_4(c \cdot e_f, 0)$. The solid line is the simulation and the dotted line is the measurements.

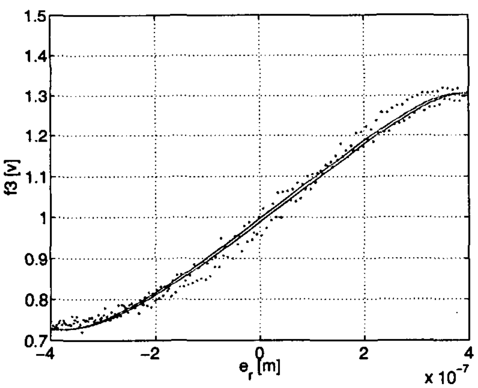

Figure 10: $f_3(0, e_r)$. The solid line is the simulation and the dotted line is the measurements.

project, which is a part of larger research project called WAVES(Wavelets in Audio Visual Electronic Systems), grant no. 56-00-0143.

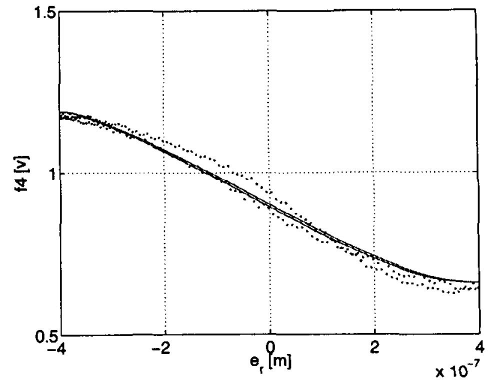

Figure 11: $f_4(0, e_r)$. The solid line is the simulation and the dotted line is the measurements.

References

[1] M. Dettori, *LMI techniques for control - with application to a Compact Disc player mechanism.* PhD thesis, Technische Universiteit Delft, The Netherlands, 2001.

[2] W. Bouwhuis, J. Braat, A. Huijser, J. Pasman, G. van Rosmalen, and K. Schouhamer Immink, *Principles of Optical Disc Systems.* Adam Hilger Ltd, 1985.

[3] E. Vidal, J. Stoustrup, P. Andersen, T. Pedersen, and H. Mikkelsen, "Open and closed loop parametric system identification in compact disk players," in *ACC2001*, (Arlington, Virginia), 2001.

[4] T.-J. Yeh and Y.-C. Pan, "Modeling and identification of opto-mechanical coupling and backlash nonlinearity in optical disk drives," *IEEE Transactions on Consumer Electronics*, vol. 46, February 2000.

[5] S. G. Stan, *The CD-ROM drive.* Kluwer Academic Publishers, 1998.

[6] E. Vidal, K. Hansen, R. Andersen, K. Poulsen, J. Stoustrup, P. Andersen, and T. Pedersen, "Linear quadratic control with fault detection in compact disk players," in *Proceedings of the 2001 IEEE International Conference on Control Applications*, (Mexico City, Mexico), 2001.

[7] E. Vidal, P. Andersen, J. Stoustrup, and T. Pedersen, "A study on the surface defects of a compact disk," in *Proceedings of the 2001 IEEE Icnternational Conference on Control Applications*, (Mexico City, Mexico), 2001.

[8] P. Odgaard, J. Stoustrup, P. Andersen, and H. Mikkelsen, "Exteded version of: Modelling of the optical detector system in a compact disc player." www.control.auc.dk/~odgaard/papers/opmodel.pdf, 2002.